On the relationship between transport and motional electric potentials in broad, shallow currents

by Thomas B. Sanford[1] and Reinhard E. Flick[2]

ABSTRACT

Knowledge of the volume transport is of great practical importance in many studies of the flow through or within shallow channels and estuaries. However, transport measurements are often difficult to obtain because of the temporal or spatial variability of the flow. The bulk motion of a stream has been inferred from measurements which integrate the electric field induced by the motion of seawater through the earth's magnetic field. Such measurements are definitely related to the spatially averaged flow, but not necessarily proportional to volume transport. In this paper are presented general expressions for the motionally induced electric potential gradient ($\nabla\varphi$) and electric current density ($\mathbf{J}/\sigma$) within a broad, shallow flow. Analog or equivalent electrical circuits and the analytical expressions are examined to determine sources of error and conditions under which useful transport measurements are possible.

The most general result for a broad, shallow stream (depth « width) gives the velocity and transport in terms of $\nabla\varphi$ at the bottom and $\mathbf{J}/\sigma$ within the water column. Such a method uniquely determines the velocity without prior knowledge of the flow and electrical conductivity structures in the region.

In the case of flow over highly conducting or thick sediments a relation between the induced potential and transport is derived. It is shown that a large sediment conductance reduces the measured signal but increases the accuracy of potential to transport conversions. High sediment conductances are common in shallow sounds, rivers and estuaries.

As an example, measurements of the potential difference across and the electric currents within the Vineyard Sound, Massachusetts, are discussed and interpreted. Large sediment conductance allowed the conversion of potential measurements into transport by a procedure based wholly on electrical measurements.

1. Introduction

Since the experiments of Faraday on the Thames River, many investigators have been intrigued by the existence of electric fields produced as water moves through the geomagnetic field. Using submarine cables, the potential differences across many straits and sounds have been observed and clearly related to water motion. Less conclusive have been attempts to relate electric measurements to water transport. The

1. Woods Hole Oceanographic Institution, Woods Hole Massachusetts, 02543, U.S.A.
2. Scripps Institution of Oceanography, La Jolla, California, 92037, U.S.A.

difficulty results from the essential fact that no unique relationship exists between generated potentials across a stream and its transport (Longuet-Higgins *et al.*, 1954).

The induced potential field depends on the spatial distribution of velocity over the bottom topography and electrical conductivity. Sufficient information about the character of the flow and measurement site is seldom available to establish an adequate theoretical relationship between potential and transport. It has been necessary to resort to idealized models of the motional induction. Such models assume that:

1. the flow is uniform and two-dimensional throughout the available channel;
2. the cross-section of the channel is simple and two-dimensional;
3. the underlying sediments are of uniform electrical conductivity and infinitely thick.

However, in most situations:

1. the flow is three-dimensional having cross- and downstream variations;
2. the bottom is irregular in shape and three-dimensional;
3. the sediments although thick compared to the water depth are thin compared with the channel width.

The usual experimental procedure is to ignore the actual situation, interpreting the flow in terms of the idealized model with direct transport calibration whenever possible. As a result most of the successful measurements are due more to the integrating character of the induction and empirical calibration than to the use of a physically adequate or applicable model.

The purpose of this paper is to propose a new observational technique capable of measuring the velocity field and hence transport in spite of ignorance about the structure and electrical conductivity of the channel. Also it is demonstrated that in a large class of naturally occurring channels known to have thick, highly conducting sediments, the induction is simpler and more useful for measuring transport than previously realized. Electrical measurements in the Vineyard Sound between Cape Cod and Martha's Vineyard Island are interpreted as an example.

2. General considerations

Within any flow of seawater electric fields and currents will be established through geomagnetic induction. The observed electric potential gradient ($\nabla\varphi$) is the combination of the source function ($\mathbf{v}x\mathbf{F}$) and the electric current response ($\mathbf{J}/\sigma$). Ohm's law for a moving medium is

$$\nabla\varphi = \mathbf{v}x\mathbf{F} - \mathbf{J}/\sigma$$

where

$\mathbf{v}$ = velocity field $\mathbf{v}(x, y, z, t)$
$\mathbf{F}$ = geomagnetic field
$\mathbf{J}$ = electric current density
σ = electrical conductivity.

For a constant and uniform geomagnetic field, the source function varies in time and space with **v**. On the other hand, the induced electric currents depend strongly on the three-dimensional structure of **v** and σ.

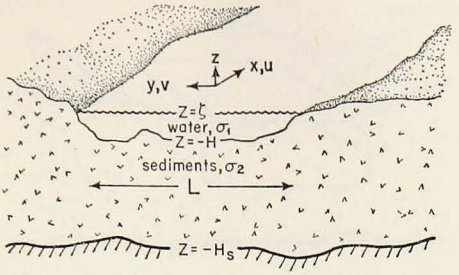

Figure 1. Model of channel and sediments.

The analytical model used in this paper consists of a flow confined to a broad, shallow channel of width L. The channel (Figure 1) has a depth of $H(x,y)$ and a free surface $\zeta(t)$. The sediments are of thickness $H_s(x,y) - H(x,y)$. The electrical conductivity structure is treated as being uniform in the flow (σ_1) and sediments (σ_2). The velocity field is horizontal (u,v) while the geomagnetic field is uniform, having components F_x, F_y, F_z.

The analysis will apply to the commonly occurring situation in which $L \gg H_s > H$. Sanford (1971) analyzed the motional induction for a laterally unbounded flow. The principal effect of channel sides is to restrict or confine the horizontally circulating electric currents. The open boundary solution can be applied with the restriction that downstream variations occurring over a scale appreciably larger than L be ignored.

The potential gradient in the flow $(-H \leqslant z \leqslant \zeta)$ is

$$\nabla\varphi = \mathbf{v}\times\mathbf{F} - \mathbf{J}/\sigma_1 \tag{1}$$

where, according to Sanford (1971), the principal electric currents are given by

$$\mathbf{J}/\sigma_1 = \nabla\times\mathbf{i}\int_z^{\zeta} F_z(\mathbf{v}-\bar{\mathbf{v}}^*)\,dz' + \frac{\bar{D}}{2\pi D}\nabla\times\mathbf{k}\int_{-\infty}^{\infty}\int \nabla\cdot F_z\bar{\mathbf{v}}^* \ln r\,dx'dy' \tag{2}$$

and in the sediments $(-H_s < z \leqslant -H)$

$$\nabla\varphi = -\mathbf{J}/\sigma_2 \tag{3}$$

where

$$\mathbf{J}/\sigma_2 = \nabla\times\mathbf{i}(H_s+z)F_z\bar{\mathbf{v}}^* + \frac{\bar{D}}{2\pi D}\nabla\times\mathbf{k}\int_{-\infty}^{\infty}\int \nabla\cdot F_z\bar{\mathbf{v}}^* \ln r\,dx'dy' \tag{4}$$

with

$r = ((x-x')^2+(y-y')^2)^{1/2}$

$D = H + \zeta + \dfrac{\sigma_2}{\sigma_1}(H_s - H)$

$\bar{D}$ = regional average of D over area of roughly L^2 in size

$\bar{\mathbf{v}}^* = \dfrac{1}{D}\displaystyle\int_{-H}^{\zeta} \mathbf{v}\,dz'$

$\mathbf{k}$ = unit vector in positive z direction.

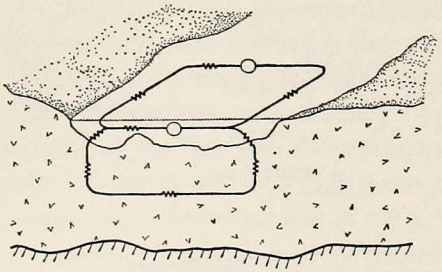

Figure 2. Schematic of equivalent circuit for motionally induced EMFs and electric currents in the vertical and horizontal planes. Circles represent voltage sources driving electric currents through lumped resistances.

Charge conservation requires that the electric currents circulate in closed loops. Driven by the high velocity portion of a flow, electric currents must return through a separate region of different velocity. Conducting sediments provide return paths which tend to increase **J** and decrease $\bar{\mathbf{v}}^*$. If the flow is assumed to be 2-dimensional, having no downstream variations, the electric currents are forced to circulate in a vertical plane. In actual flows, currents also circulate in loops in the horizontal plane. Equations (2) and (4) and Figure 2 describe both modes of circulation.

It should be emphasized that the induction is dominated by the conductivity-weighted average velocity. The variable D is equal to the equivalent depth of water having the same conductance as the water plus sediments. It will be useful later to introduce the parameter β:

$$\beta = \frac{\sigma_1}{\sigma_2(H_s - H)}.$$

Then

$$\bar{\mathbf{v}}^* = \frac{\beta(H+\zeta)}{1+\beta(H+\zeta)}\bar{\mathbf{v}}, \tag{5}$$

where

$$\bar{\mathbf{v}} = \frac{1}{H+\zeta}\int_{-H}^{\zeta} \mathbf{v}\,dz.$$

In the case of sediments which are thin or of low electrical conductivity, $\beta H \gg 1$. Then $\bar{\mathbf{v}}^*$ is about equal to $\bar{\mathbf{v}}$. On the other hand, over sediments of high relative conductance $\beta H \ll 1$ and $\bar{\mathbf{v}}^*$ is equal to $\beta(H+\zeta)\bar{\mathbf{v}} \ll \bar{\mathbf{v}}$.

a. Electric currents in the vertical plane. The first term in (2) and (4) describing **J** in the flow results from electric currents circulating in the vertical plane. These currents are largely horizontal due to the restriction that $L \gg H_s$ and are of a local origin. The local generation arises because lateral boundaries have little influence on these electric currents. The potential gradient observable is

$$\left.\begin{aligned} \frac{\partial \varphi}{\partial x} &= F_z \bar{v}^*, \\ \frac{\partial \varphi}{\partial y} &= -F_z \bar{u}^*. \end{aligned}\right\} \tag{6}$$

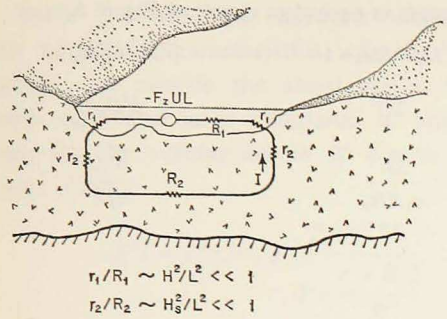

Figure 3. Equivalent electric network for induction in a vertical plane.

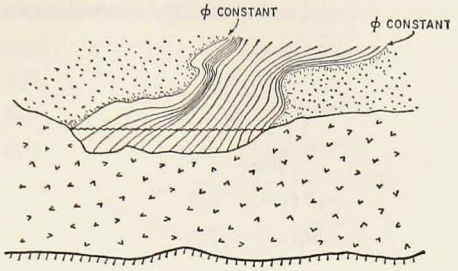

Figure 4. Lateral boundaries and depth contours for a channel having a narrows or constriction. In this case flow streamlines and depth contours change together such that $\bar{\mathbf{v}}^* \cdot \nabla D = 0$ everywhere.

Figure 3 presents a network equivalent to illustrate how the conductivity weighting arises. Let U be a typical velocity and for simplicity ignore ζ. Then for $L \gg H_s > H$, the vertical resistances are small compared with the horizontal resistances and can be ignored.

Then the electric current per unit distance downstream in the equivalent circuit is

$$I = \frac{-F_z U \sigma_1 H}{1 + \dfrac{\sigma_1 H}{\sigma_2 (H_s - H)}}.$$

The potential difference across the flow is

$$\Delta\varphi = -F_z UL - \frac{L}{\sigma_1 H} I = -\beta H \frac{F_z UL}{1 + \beta H}.$$

This result is equivalent to (5) and (6) and illustrates the effect of conducting sediments in reduc ng the average induced potential difference measured on submarine cables. It is precisely this shunting which necessitates measuring or assuming the conductivity structure of the sediments or relying on direct calibration schemes when cable measurements of induced voltage alone are used to infer transport.

b. Electric currents in the horizontal plane. The second term in (2) and (4), denoted simply as **J*** henceforth, describes currents circulating in the horizontal plane. The strength and scale of these currents are determined by the three-dimensional variations of $\nabla \cdot \bar{\mathbf{v}}^*$, which in turn depends on the structure of the flow and the electrical conductivity of the water and channel. The circulation is essentially horizontal at all depths in the water and sediments. Lateral boundaries tend to inhibit these large-scale electric currents.

Loops of electric current will arise in the vicinity of topographic features such as

Table I. General and specialized expressions for elements in equivalent circuit of Figure 5.

	$\beta' H_0 \sim \beta H_0 \gg 1$	$\beta' H_0 \leqslant \beta H_0 \ll 1$
In shoal region		
$\bar{U}^* \simeq \dfrac{\beta' H_0 \bar{U}}{1 + \frac{1}{2}\beta' H_0}$	$2\bar{U}$	$\beta' H_0 \bar{U}$
$R' \simeq \dfrac{\beta' L}{\sigma_1 X (1 + \frac{1}{2}\beta' H_0)}$	$\dfrac{2L}{\sigma_1 X H_0}$	$\dfrac{\beta' L}{\sigma_1 X}$
$\beta' \simeq \sigma_1/\sigma_2 (H_s - \frac{1}{2} H_0)$		
Outside shoal region		
$\bar{U}^* \simeq \dfrac{\beta H_0 \bar{U}}{1 + \beta H_0}$	$\bar{U}$	$\beta H_0 \bar{U}$
$R \simeq \dfrac{\beta L}{\sigma_1 X (1 + \beta H_0)}$	$\dfrac{L}{\sigma_1 X H_0}$	$\dfrac{\beta L}{\sigma_1 X}$
$r \simeq \dfrac{\beta X}{\sigma_1 L (1 + \beta H_0)}$	$\dfrac{X}{\sigma_1 L H_0}$	$\dfrac{\beta X}{\sigma_1 L}$
$\beta \simeq \sigma_1/\sigma_2 (H_s - H_0)$		
Conductivity weighted velocity difference		
$\Delta \bar{U}^* = \bar{U}^*_{(\text{shoal})} - \bar{U}^*_{(\text{outside})}$	$\bar{U}$	$-\dfrac{\sigma_1 H_0^2}{2\sigma_2 H_s^2} \bar{U}$

shoals and ridges. Yet a lateral constriction of the flow unaccompanied by depth changes will not produce **J*** currents. According to (2), **J*** is generated in regions in which $\nabla \cdot \bar{\mathbf{v}}^* \neq 0$. The role of D is clearly evident when $\nabla \cdot \bar{\mathbf{v}}^*$ is expressed in terms of depth changes.[1]

$$\nabla \cdot \bar{\mathbf{v}}^* = -\frac{1}{D}\frac{\partial \zeta}{\partial t} - \frac{\bar{\mathbf{v}}^*}{D} \cdot \nabla D.$$

Consider a steady flow through the channel shown in Figure 4 in which the equivalent depth, D, is uniform along transport streamlines. Then $\bar{\mathbf{v}}^* \cdot \nabla D = 0$; no **J*** currents exist and the channel sides are equipotentials.

Osgood *et al.* (1970) designate **J*** as currents of type 1. Their estimate of **J*** in the vicinity of a narrows in the English Channel is based on the concentration or acceleration of flow approaching the constriction. Although changes to $\bar{\mathbf{v}}^*$ have a role, it is secondary to that played by ∇D.

However, there is little doubt that **J*** induction is important in many situations. As written in (2), **J*** is difficult to evaluate, especially in channels. So consider an analog circuit shown in Figure 5. The channel of width L and depth H_0 has a ridge or shoal of depth $\frac{1}{2} H_0$ and width X.

[1] Where the conditions that $\nabla \cdot \mathbf{v} = 0$ in the flow, that the flow normal to the bottom vanishes $(\mathbf{v} \cdot \mathbf{n}(-H) = 0)$ and that at the free surface $\mathbf{v} \cdot \mathbf{n} = \partial\zeta/\partial t$ are used. The vertical component of velocity is assumed to be negligible compared with the horizontal components, but is non-zero.

Table I relates the network elements to the physical characteristics of the channel within and outside the shoal region for βH_0 both small and large compared to unity. Solving for the voltage across R' due to J_y^* currents yields

$$R'I = J_y^* L/\sigma_1 \simeq \frac{F_z \Delta \bar{U}^* L}{1 + \dfrac{r + R/2}{R'}}$$

The ratio of $\mathbf{J}^*/\sigma_1$ and $\Delta\varphi$ [from (6)] is the relative error in potential measurements due to ignored $\mathbf{J}^*$ electric currents.

According to Table I, the relative magnitude of J_y^*/σ_1 in the shoal region for $\beta H_0 \gg 1$ is

$$\frac{J_y^*/\sigma_1}{-F_z \bar{U}^*} \simeq \frac{1}{\dfrac{5}{2} + \dfrac{X^2}{L^2}}.$$

Similarly for $\beta H_0 \ll 1$ the result is

$$\frac{J_y^*/\sigma_1}{-F_z \bar{U}^*} \simeq \frac{-H/H_s}{3 + \dfrac{2X^2}{L^2}}.$$

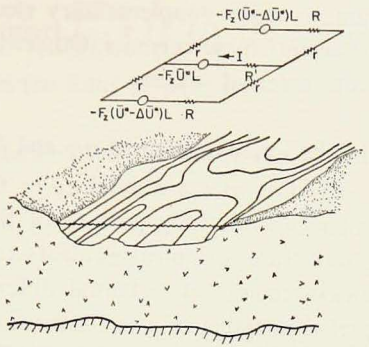

Figure 5. Lateral boundaries and depth contours for a channel having a localized shoal and the equivalent electric network for induction in a horizontal plane.

As expected, the influence of $\mathbf{J}^* \to 0$ as the current paths are elongated for increasingly larger X/L. For small X/L and $\beta H_0 \gg 1$, $\mathbf{J}^*/\sigma_1$ gradients approach 40% of $F_z \bar{U}^*$. Thus a cable across the shoal would measure $-F_z(1-.4)\,\bar{U}^* L$. The reduction in expected voltage is commonly, but in this case erroneously, ascribed to currents in the vertical plane.

Regardless of X/L, $\mathbf{J}^*$ is not significant for $\beta H_0 \ll 1$; since $\sigma_1/\sigma_2 > 1$, H_s must be much greater than H_0. It is interesting to note that $\mathbf{J}^*$ currents actually increase the potential across the shoal.

Estimates of $\mathbf{J}^*$ currents can be made from potential difference measurements along the shore line (path r in Figure 5).

Electric currents not generated by the local velocity field but of external origin can produce strong and variable background electric fields. These magnetotelluric or earth currents are produced generally by temporal variations of the geomagnetic field, but they can also arise from strong water motion outside the measurement site. In general, these currents behave like $\mathbf{J}^*$ currents, being horizontal and distributed in the water and sediments in proportion to conductivity. In most cases, it is impor-

tant to make supplementary electric measurements, away from the local flow, to determine these currents. Otherwise, the desired measurements may be contaminated from external sources.

3. The interpretation of $\nabla\varphi$ and $\mathbf{J}/\sigma$ with application to channels having $\beta H < 1$.

The flux of sea water into or through an experimental region is often difficult to determine for long periods of time by any known method. For this reason even crude transport measurements can be of considerable value. With mixed success, measurements of potential differences across streams have been made and interpreted in terms of water transport. The principal difficulty with this method is that the electrical response is a complicated function of the spatial structure of the velocity field and electrical conductivity of the water and sediments. The behavior of (2) revealed by the analog network examples of Section 2 serves to estimate only crudely the electrical response within a flow. More refined transport estimates require either considerable prior knowledge about $\mathbf{v}$ and σ or extensive electrical measurements or simplification of (2). The purpose of this section is to examine how to estimate transport without extensive prior knowledge of the distribution of $\mathbf{v}$ and σ.

The Appendix shows that simultaneous measurements of both electric fields and electric currents within a broad, shallow stream can be used to determine the velocity field in spite of ignorance about the characteristics of the measurement site. Although offering considerable promise, the method outlined in the Appendix has not been utilized as yet and is not well suited for transport measurements for long periods of time. Thus further discussion of this method appears in the Appendix so that the emphasis of this section can remain on potential difference and electric current measurements.

The network analysis of Section 2 shows that $\mathbf{J}^*$ currents are negligible when $\beta H \ll 1$, resulting from $H/H_s \ll 1$, or when $X/L \gg 1$, since $\nabla \cdot \bar{\mathbf{v}}^* \to 0$. Ignoring $\mathbf{J}^*$ currents, (1), (2), and (5) can be integrated to yield

$$\Delta\varphi = \int \frac{\partial \varphi}{\partial y}\, dy = -F_z \int \beta \frac{(H+\zeta)\bar{u}}{1+\beta(H+\zeta)}\, dy \tag{7}$$

$$\int_{-H}^{\zeta}\int \frac{J_y}{\sigma_1}\, dydz = F_z \int \frac{(H+\zeta)\bar{u}}{1+\beta(H+\zeta)}\, dy \tag{8}$$

where the indefinite integral, $\int(\,)dy$, indicates integration across the flow. Similarly, from (2) and (5) the transport can be expressed as

$$Q = \frac{1}{F_z}\int_{-H}^{\zeta}\int (1+\beta(H+\zeta))J_y/\sigma_1 dzdy. \tag{9}$$

For a flow which is essentially uniform downstream $\left(\frac{X}{L} \gg 1\right)$, (7), (8), and (9) are valid for all β and can be easily evaluated in the limit of βH either small or large compared to unity.

It is possible but unlikely that σ_2 is ever greater than σ_1. Hence, the condition that $\beta H \ll 1$ also states that $H/H_s \ll 1$. In this case

$$\beta \simeq \frac{\sigma_1}{\sigma_2 H_s}. \tag{10}$$

Moreover, when β is uniform along the path of integration, it can be brought outside the integral of (7) with the result that

$$\beta = \frac{-\Delta\varphi}{\int\int_{-H}^{\zeta} J_y/\sigma_1 dzdy}. \tag{11}$$

The transport in this case is given as

$$Q = \frac{-1}{\beta F_z}\left[\Delta\varphi - \beta^2 \int\int_{-H}^{\zeta} (H+\zeta) J_y/\sigma_1 dzdy\right]. \tag{12}$$

Substituting from (11) for one of the β's appearing inside the brackets in (12) yields

$$Q = \frac{-\Delta\varphi}{\beta F_z}[1 + \beta\tilde{H}] \tag{13}$$

where

$$\tilde{H} = \frac{\int\int_{-H}^{\zeta} (H+\zeta) J_y/\sigma_1 dzdy}{\int\int_{-H}^{\zeta} J_y/\sigma_1 dzdy}. \tag{14}$$

Equations (11) and (14) allow β and $\tilde{H}$ to be evaluated from the measurement of the potential difference across and the electric current within a stream. To the authors' knowledge electric current profiles have never been taken in order to calibrate a submarine cable. In a few instances measurements of the voltage between towed electrodes, the G.E.K. method (von Arx, 1950), have been made near submarine cables. The towed electrodes of the G.E.K. method are advected by the surface current and sense an apparent voltage gradient equal to $-\mathbf{J}/\sigma_1$ (Longuet-Higgins *et al.*, 1954). Hughes (1962) and Teramoto (1971) have combined cable and G.E.K. data to estimate the conductance of the sea floor. This approach, which is also used later in this section, is most useful when the flow is uniform with depth; then J_y/σ_1 is independent of depth and need only be measured at the sea surface.

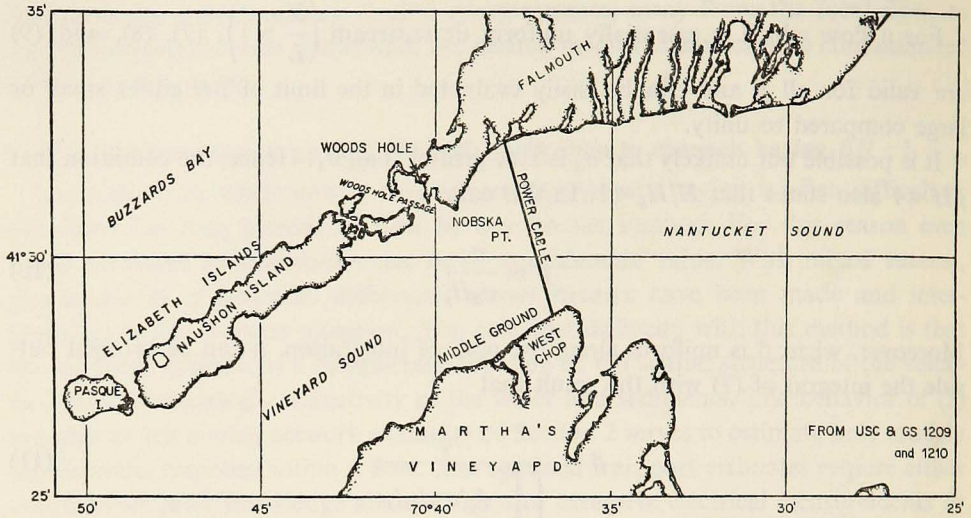

Figure 6. Chart of Vineyard and Nantucket Sounds showing position of submarine cable.

Conventionally, regions in which $\beta\tilde{H} < 1$ are considered poor measurement sites because the sediments greatly reduce the measurable potential differences and the interpretation is highly dependent on the generally unknown sediment conductance. However, situations in which $\beta H < 1$ are common, especially in shallow coastal sounds. Bowden and Hughes (1961) and Vaux (1955) report measurements in the southern North Sea over and near the Aldeburgh-Domburg submarine cable where $\beta H = .17$. Düing (1965) determined the equivalent of $\beta H = .36$–$.58$ over channels into the Gulf of Naples. Teramoto (1972) found $\beta H = .11$ in the Tsugaru Straits. To the extent that the measurement situation complies with the assumptions of this section, the present results show that the conductance is measurable and that the reduction in signal strength accompanies an increase in the accuracy of transport determinations.

a. Electric measurements on the Vineyard Sound. Experiments to monitor transport were conducted near Woods Hole, Massachusetts, within a flow of small $\beta\tilde{H}$. In the summer of 1969 the potential differences and electric currents were measured across the Vineyard Sound between Falmouth and West Chop on Martha's Vineyard (Figure 6). During the period of electrical measurements, surface and subsurface drogues were tracked and drift bottles and seabed drifters were released by Bumpus, Wright and Vaccaro (1971). The purpose of these measurements was to estimate the flux of sea water in the Vineyard Sound as a whole and near a proposed sewage outfall in particular.

Potential measurements were made on a spare electric power cable provided by the courtesy of the New Bedford Gas and Edison Electric Co. (formerly the Cape

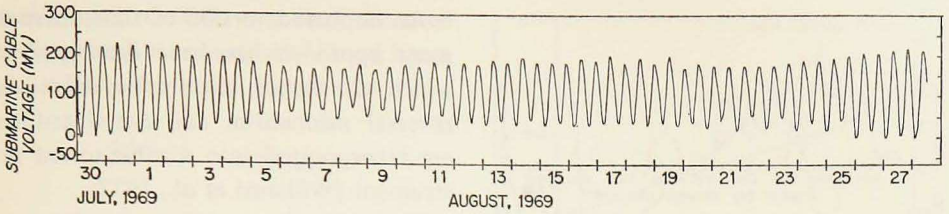

Figure 7. Potential differences across the Vineyard Sound. Higher voltages (positive fluctuations) result from increased eastward flow.

and Vineyard Electric Co.). On the Falmouth side, the center conductor of the cable was grounded, while at West Chop the voltage between the center conductor and West Chop local ground was recorded on a strip chart recorder. Access to the submarine cable was inland about 150 m at each end. It was not possible to deploy electrodes on the shoreline connected by additional cables back to the power company's facilities. The power company grounds were well established, having been in place for many years, yet contributed a bias to the measurements shown in Figure 7 of about +110 mv. The long-term stability of the bias can be determined by G.E.K. measurements, as discussed next, or by making the potential measurements with stable electrodes between opposite shorelines.

To determine the cable bias, β and $\tilde{H}$, 14 G.E.K. transects were made on four separate days. The G.E.K. measurements were obtained by a method first developed by Mangelsdorf (1962) in which seawater-filled tubes of different lengths are towed behind a vessel. The tubes, of 2 cm (.75 inch) I.D. polyethylene, were 60 and 30 m in length and were plugged with Vycor, a porous glass. The Vycor plug maintained electrical contact with the seawater but allowed the inboard ends of the tubes to come directly aboard the vessel and into its laboratory. The potential difference between the seawater at the inboard ends is equal to that conventionally measured by G.E.K. electrodes located at the outboard ends.

Rather than placing electrodes directly within the seawater at the inboard ends of the towed tubes, we inserted a second pair of seawater-filled tubes connected to a pair of electrodes in a Dewar flask. Each tube of this pair was a closed seawater-filled tube contained at one end with a silver-silver chloride electrode and at the other end with a Vycor plug. Thus each electrode was at the end of a continuous, conducting path of seawater extending either 30 or 60 m behind the vessel. This scheme allowed the electrodes to remain in a thermally stable environment and yet able to be connected alternately to the longer or shorter towed tube. Periodic reversal of the electrodes showed that the slow drift of the electrode bias never exceeded 0.1 mv on a given transect.

The potential between the electrodes was measured by an extremely high input-impedance electrometer (Keithley Instruments, model 602). In order to reduce noise due to surface wave and boat wake, a low-pass filter was used between the output of the electrometer and the strip chart recorder.

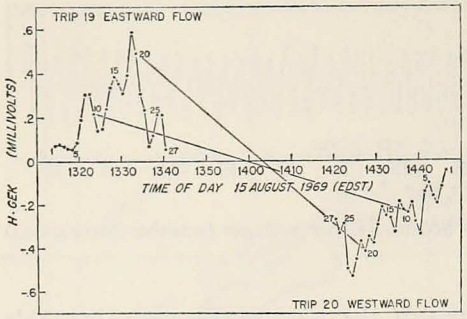

Figure 8. Measurements of H·GEK across the Sound before and after slack water. Numerals refer to positions along the G.E.K. transect between Falmouth and West Chop.

An improved version of this measurement approach has been developed in which the tubes, electrodes, electrode reversal mechanism and amplifier-filter are incorporated into a cable-towed instrument (Williams *et al.*, 1972).

Slack-tide times and hence cable zero were determined by plotting the G.E.K. voltage gradient times the depth at stations across the Sound versus time of day for two G.E.K. transects; the first of which was taken before current reversal, the second after. In Figure 8 run # 19 was completed during easterly flow and run # 20 during westerly flow. By means of fathometer readings taken during the G.E.K. runs, it was possible to correlate time of day and position across the Sound, and, hence, to deduce the times during each run that the boat was at a given position. The numbers 1–27 next to the data points in Figure 8 indicate the positions of the G.E.K. measurements made during the two succeeding runs. By connecting pairs of points with the same position number, the time of slack water at that place can be read from the horizontal axis. This procedure assumes that the flow transition occurs linearly with time and that the G.E.K. voltage measured at the surface is proportional to the tidal transport averaged over depth at that location. That the flow speed is nearly uniform with depth is verified by drogue measurements over a period of several hours (Bumpus *et al.*, 1971). Near the time of slack water, however, the flow may not be uniform in the vertical.

The times of slack water determined by this procedure are shown in Figure 9. From these data the time of 1355 is taken as the time of average slack water across the G.E.K. transect. The large cross-stream variability is consistent with the observation of Redfield (1953) that tides in this area are dominated by the interference of two oppositely-directed progressive waves. In the submarine cable area, the interference results in a small tidal range, which allows ζ to be ignored, and in closely packed cotidal lines, which leads to large tidal phase differences over small distances. In this last respect the present cable was not well suited to G.E.K. calibration.

The cable voltage, $\Delta\varphi$, is taken as the difference between the measured cable voltage at any time and the cable voltage measured at slack tide. Positive voltages, representing a positive potential gradient across the Sound from south to north, imply eastward flow. On both 14 and 15 August the slack tide voltage was the same but 15 mv more positive than that observed on 31 July. It is thought that this 15 mv change in bias results from the grounds used.

Once the slack tide voltage was known, the average cable voltage, $\Delta\varphi$, measured

during each G.E.K. run could be used to compute β via equation (11) and hence to calibrate the cable. Recall that

$$\frac{J_y(y,\zeta)}{\sigma_1} = -\,\mathrm{GEK}(y)$$

where GEK(y) stands for the voltage gradient measured at the sea surface between a pair of towed electrodes. If the flow speed is uniform with depth, as has already been assumed, so will be the G.E.K. voltage gradient. Hence

$$\int\int_{-H}^{\zeta} J_y/\sigma_1 dz dy = -\int (H+\zeta)\,\mathrm{GEK}\,dy$$

and therefore

$$\beta = \frac{\Delta\varphi}{\int (H+\zeta)\,\mathrm{GEK}\,dy}. \qquad (15)$$

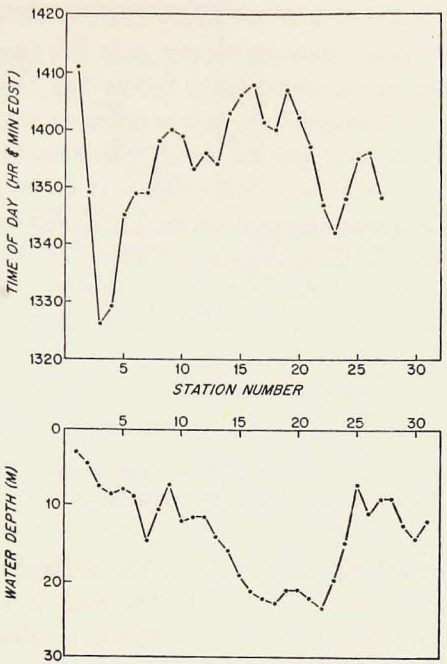

Figure 9. Time of slack water (upper panel) and water depth (lower panel) versus position across the Vineyard Sound.

The determination of β and the cable calibration factor is made by fitting a line to the data plotted in Figure 10 which shows the submarine cable voltage plotted versus the $\int H \cdot \mathrm{GEK}\,dy$. The size of each box reflects the estimated uncertainties in the cable and G.E.K. measurements. In both cases, the scale of the box results from an expected error of $\pm 1\%$ of full scale on the recorders and from the fact that the G.E.K. runs required $\frac{1}{2}$ hour to complete. The tidal range, $\zeta(t)$, is less than 0.5 m everywhere in the cable area and was neglected in the computation.

Runs 5 and 6 indicate values of $\int H \cdot \mathrm{GEK}\,dy$ which are 30% too small compared with the other data. A possible explanation for this discrepancy may be that during these two runs the flow was at a maximum toward the west and the winds were 8–15 knots out of the southwest to west. Blowing opposite to the direction of the current, the wind produced much sea surface chop. The increased wind drag, producing the choppy sea, might have reduced the near surface current speed relative to the deeper water, and, thereby have reduced the G.E.K. voltage gradient. On no other G.E.K. runs were the current and wind both strong and in opposite directions. The direct action of the wind on the vessel should contribute no signal to the G.E.K. measurement (Longuet-Higgins *et al.*, 1954).

A straight-line fit to this data has a slope, β, of 0.019 m^{-1}. Computation of the ratio

$$\tilde{H} = \frac{\int H^2 \cdot \mathrm{GEK}\,dy}{\int H \cdot \mathrm{GEK}\,dy}$$

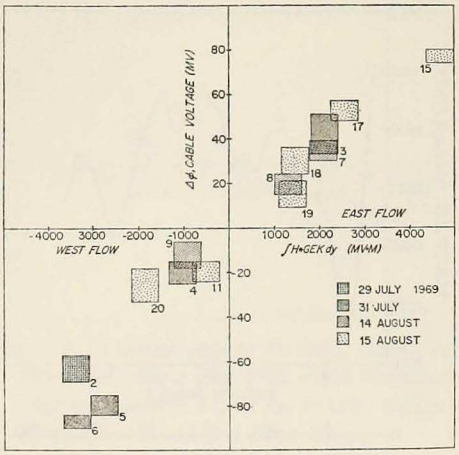

Figure 10. Plot of cable voltage versus $\int H \cdot$ GEK dy for 14 G.E.K. transects.

gave a mean value of $\tilde{H} = 17.8$ m and, hence, a $\beta\tilde{H}$ of .34 for the Sound. This value for $\tilde{H}$ was very stable, having a standard deviation from the mean of only 1.6 m over the 14 G.E.K. transects. The average depth $\bar{H}$ across the Sound at the cable location is slightly less, $\bar{H} \simeq 14.5$ m. This discrepancy arises from the larger weighting of deeper depths by the H^2 term in the integral in the numerator. Assuming $F_z = -0.5 \times 10^{-4}$ weber/m^2 substitution into equation (13) gives a calibration factor $Q/\Delta\varphi = 1400$ m^3/sec/mv for the submarine cable.

The measured value of $\beta\tilde{H}$ compares well with that estimated from geological knowledge of the region. The average water depth is 15 m with an underlying sediment layer 150 m thick. The ratio σ_1/σ_2 was measured to be 3 from a core of the sand and gravel bottom. Hence, a value of $\beta\bar{H} \simeq .3$ was expected prior to the measurements.

The voltage fluctuations of Figure 7 indicate that the peak tidal transport varied from about 160×10^3 m^3/sec during spring tides to about 70×10^3 m^3/sec during neap tides. Using the G.E.K. transects, the cable voltages corresponding to zero transport were determined to be +96 mv on 31 July and +111 mv on 14–15 August 1969. Computation of the average flood and ebb and net transports during 4 semidiurnal tidal cycles on 14 and 15 August yielded average transports of 1.3×10^9 m^3 to the west and 1.8×10^9 m^3 to the east, for a net transport of $.5 \times 10^9$ m^3 of water to the east, per semidiurnal tidal cycle. Similar calculations for 2 cycles during 30–31 July gave transports of 1.6×10^9 m^3 to the west and 2.4×10^9 m^3 to the east per tidal cycle, with a net transport of 0.8×10^9 m^3 to the east per cycle. We regard the estimate of 14–16 August with more confidence since two determinations of slack tide were made at that time, while the 30–31 July calculations rest on only one determination, as outlined previously.

4. Conclusions

We have developed a framework within which to interpret simultaneous measurements of $\Delta\varphi$ and $\mathbf{J}/\sigma_1$ across broad, shallow flows over thick, highly conducting sediments. In particular, we have shown how potential measurements on a submarine cable can be related to water volume transport using simultaneous towed electrode potential (G.E.K.) measurements to arrive at the cable calibration.

A major source of error in relating submarine cable potentials to volume transport

is the existence of large-scale horizontal electric currents which we have shown are small for sites with small $\beta\tilde{H}$. For areas of small $\beta\tilde{H}$, then, the serious errors in cable calibration arise (1) from the changes in water and seabed conductivity across the flow, with depth, or with time, and (2) from the assumption that the horizontal flow is uniform with depth. The method of towed electrodes offers no way around the latter assumption. A free fall G.E.K. system which avoids this limitation is outlined in the Appendix. More serious are spatial and temporal changes in conductivity, for then the parameter β is no longer constant and the simplifying steps leading to equation (13) are no longer possible. Estuaries and other areas of large fresh water outflow have high vertical conductivity gradients that may also change with time so that the simple relations presented here may not apply.

In areas where the conductivity is reasonably constant, it should be emphasized that even if β is not known, transport can still be monitored in a relative sense. Alternate methods could be used to determine Q which would then determine β. If the conductivity structure is known, say from geological information, β can be estimated. The method used under appropriate circumstances has the advantages that it measures transport for long periods of time, inexpensively and with no impedance to flow or vessels.

Appendix. Transport measurements using $\nabla\varphi$ and $\mathbf{J}/\sigma$

A technique is proposed to determine the velocity field within a broad, shallow stream from measurements of the potential gradient and electric current density.

For horizontal velocity, Ohm's law can be written as

$$\mathbf{v} = \frac{1}{F_z}\mathbf{k}\mathbf{x}(\nabla\varphi + \mathbf{J}/\sigma)\,. \tag{A1}$$

Equation (A1) holds regardless of the characteristics of the flow, bottom topography or water and sediment conductance. Thus measurements of $\nabla\varphi(y,z)$ and $\mathbf{J}/\sigma(y,z)$ across the stream would determine the velocity field and hence the transport. In practice, the measurement of $\nabla\varphi$ is difficult to obtain since it must be measured by stationary electrodes. On the other hand, measurements of $\mathbf{J}/\sigma$ can be readily made of the voltage between horizontally-spaced electrodes mounted on a falling probe free to move horizontally with the flow. Such an instrument observes an apparent electric field given by $-\mathbf{J}/\sigma$ (Longuet-Higgins *et al.*, 1954).

However, the difficulty in making $\nabla\varphi$ measurements is greatly reduced within flows broad compared with the water and sediment depths. In this case the potential gradient is essentially independent of depth, hence measurable on the channel bottom. From (2) $\mathbf{J}/\sigma_1$ is given as

$$J_y/\sigma_1 = -F_z(u-\bar{u}^*) + J_y^*/\sigma_1. \tag{A2}$$

Hence from (1)

$$\frac{\partial\varphi}{\partial y} = -F_z\bar{u}^* - J_y^*/\sigma_1. \tag{A3}$$

Adding (A2) and (A3) yields

$$\frac{\partial\varphi}{\partial y} + J_y/\sigma_1 = -F_z u. \tag{A4}$$

The transport across the stream is

$$Q = -\frac{1}{F_z}\left[\int (H+\zeta)\frac{\partial \varphi}{\partial y}\,dy + \int\int_{-H}^{\zeta} J_y/\sigma_1 dz dy\right]. \tag{A5}$$

Equation (A5) is similar to Hughes' (1962) equation (10) except that he brought the factor $(H+\zeta)$ outside the integral. Not incorporating $H(y)$ in the integration will lead to significant errors in channels having large cross-stream depth variations such as North Channel studied by Hughes (1962).

Spatial variations of σ do not affect the use of this approach. For the general case of a continously variable σ, the subscripts on σ can be dropped. In this case

$$\bar{\mathbf{v}}^* = \frac{\int_{-H}^{\zeta} \sigma \mathbf{v}\,dz'}{\int_{-H_s}^{\zeta} \sigma\,dz'}. \tag{A6}$$

The electric current density is given by

$$\mathbf{J} = \nabla \mathbf{x} \int_{z}^{\zeta} \sigma F_z(\mathbf{v} - \bar{\mathbf{v}}^*)\,dz' + \mathbf{J}^*. \tag{A7}$$

When combined (A7) and (1) yield (A4) except that σ_1 is replaced by σ which is now variable.

This method is being actively applied in the deep ocean (Drever and Sanford, 1970). A free-fall probe is used to measure and record $\mathbf{J}/\sigma$ and another moored instrument measures $\nabla\varphi$ near the sea floor. For use in shallow water, a modification of this approach would be capable of measuring with one device $\mathbf{J}/\sigma$ with depth and $\nabla\varphi$ on the sea floor. Such measurements at a number of stations across a stream would determine the transport.

Acknowledgements. The authors wish to thank the New Bedford Gas and Edison Electric Company for making the submarine cable available for our use. We are particularly indebted to Harry Rayment, John Branch, and David Dunham of the electric company and to Arthur Colburn of the vessel *Asterias* for their efforts and cooperation. One of us, R.E.F., greatly benefitted from being at Woods Hole as a summer Student Fellow in 1969 and is grateful for this opportunity. Also, we are indebted to Paul Mangelsdorf and Myrl Hendershott for reading the manuscript and for suggesting a number of improvements. This work was conducted with financial support from the Office of Naval Research under contract N00014-66-CO241 NR 083-004.

REFERENCES

Bowden, K. F., and P. Hughes. 1961. The flow of water through the Irish Sea and its relation to wind. Geophys. J., *4*(5): 265–291.

Bumpus, Dean F., W. Redwood Wright and Ralph F. Vaccaro. 1971. Sewage disposal in Falmouth, Massachusetts, II. Predicted effect of the proposed outfall. J. Boston Soc. Civ. Eng., *58*(4): 255–277.

Drever, R. G., and T. B. Sanford. 1970. A free-fall electromagnetic current meter – instrumentation. Proc. of the I.E.R.E. Conference on Electronics in Ocean Technology, 8–9 Bedford Square, London; pp. 353–370.

Düing, Walter. 1965. Strömungsverhältnisse im Golf von Neapel. Sonderdruck aus Pubbl. staz. zool. Napoli, *34:* 256–316.

Hughes, P. 1962. Towed electrodes in shallow water. Geophys. J. Roy. Astr. Soc., *7*(1): 111–124.

Longuet-Higgins, M. S., M. E. Stern and Henry Stommel. 1954. The electrical field induced by ocean currents and waves, with application to the method of towed electrodes. Pap. Phys. Oceanogr. and Meteorol., *13*(1): 1–37.

Mangelsdorf, P. C., Jr. 1962. The world's longest salt bridge. In: Marine Sciences Instrumentation, Vol. *1*, Plenum Press, New York: 173–185.

Osgood, C., W. G. V. Rosser and N. J. W. Webber. 1970. Electric and magnetic fields associated with sea tides in the English Channel. Phys. Earth Planet. Interiors, *4:* 65–77.

Redfield, A. C. 1953. Interference phenomena in the tides of the Woods Hole region. J. Mar. Res., *12*(1): 121–140.

Sanford, Thomas B. 1971. Motionally induced electric and magnetic fields in the sea. J. Geophys. Res., *76*(15): 3476–3492.

Teramoto, Toshihiko. 1971. Estimation of sea-bed conductivity and its influence upon velocity measurements with towed electrodes. J. Oceanogr. Soc. Japan, *27*(1): 7–18.

Vaux, David. 1955. Current measuring in shallow waters by towed electrodes. J. Mar. Res., *14*(2): 187–194.

von Arx, W. S. 1950. An electromagnetic method for measuring the velocities of ocean currents from a ship under way. Pap. Phys. Oceanogr. and Meteorol., *11*(3): 1–62.

Williams, A. J., III, R. J. Jaffee, P. F. Poranski, and P. J. Simonetti. 1972. Short arm electric field measurements of ocean currents. Woods Hole Oceanographic Institution Technical Report No. 72–13 (unpublished manuscript): 80 pp.

Received: *4 February, 1974*; revised: *1 August, 1974.*
Contribution No. 3270 from the Woods Hole Oceanographic Institution.